Int. J. Electrochem. Sci., 11 **(2016)** 8439 – 8446, doi: 10.20964/2016.10.60

International Journal of ELECTROCHEMICAL SCIENCE
www.electrochemsci.org

ZnO Nanorods Grown Directly on Copper Foil Substrate as a Binder-Free Anode for High Performance Lithium-Ion Batteries

Lanyan Huang[1,5], *Xin Wang*[1,*], *Fuxing Yin*[2,3], *Yongguang Zhang*[2,3,*], *Jinwei Gao*[5], *Junming Liu*[5], *Guofu Zhou*[1] *and Zhumabay Bakenov*[2,4]

[1] Institute of Electronic Paper Displays, South China Academy of Advanced Optoelectronics, South China Normal University, Guangzhou, Guangdong Province, China.
[2] Synergy Innovation Institute of GDUT, Heyuan, Guangdong Province, China
[3] Research Institute for Energy Equipment Materials, Tianjin key laboratory of laminating fabrication and interface control technology for advanced materials, Hebei University of Technology, Tianjin 300130, China
[4] Institute of Batteries LLC, Center of Energy and Advanced Materials Science, PI National Laboratory Astana, School of Engineering, Nazarbayev University, 53 Kabanbay Batyr Avenue, Astana 010000, Kazakhstan
[5] Institute of Advanced Materials, South China Academy of Advanced Optoelectronics, South China Normal University, Guangzhou, Guangdong Province, China.
[*]E-mail: yongguangzhang@hebut.edu.cn; wangxin@scnu.edu.cn

Received: 4 July 2016 / *Accepted:* 29 August 2016 / *Published:* 6 September 2016

ZnO nanorods directly grown on copper foil substrate were obtained via hydrothermal method without using templates. Structure and morphology of the as-prepared ZnO nanorods were characterized by X-ray diffraction, scanning electron microscopy and high-resolution transmission electron microscopy. The ZnO nanorods on copper foil (ZnO@CF) exhibited remarkably enhanced performance as anode for lithium batteries with the initial discharge capacity of 1236 mAh g^{-1} and a capacity of 402 mAh g^{-1} retained over 100 cycles at a current density of 200 mA g^{-1}. The ZnO@CF anode demonstrated an excellent rate capability, delivering a reversible capacity of 390 mAh g^{-1} at 1500 mA g^{-1}. This superior performance of the ZnO@CF anode is believed to be due to the unique structure of this binder-free anode, favoring mass and charge transfer at its interface with the electrolyte, effectively reducing the Li-ions diffusion paths and providing conditions to accommodate the anode volume variations upon charge-discharge cycling.

Keywords: Lithium ion battery, Anode, ZnO nanorods, Binder-free

1. INTRODUCTION

Graphite, which is widely used as anode for the lithium-ion batteries (LIBs), has a limited theoretical capacity of 372 mAh g^{-1}[1]. The transition metal oxides (Fe_3O_4, NiO and Co_3O_4 etc.) are considered as promising alternative anode materials for LIBs due to their high theoretical capacities, low cost and environmental friendliness[2,3]. Among them, ZnO could be especially attractive due to its high theoretical capacity of 978mAh g^{-1}, natural abundance, easy preparation and chemical stability[4,5]. However, ZnO anode suffers from severe capacity fading due to its poor conductivity and large volume variation (about 300%) during discharge and charge leading to its mechanical disintegration.

To overcome these problems, efforts were centered on material design and optimization of preparation techniques to obtain favorable architecture of ZnO, e.g. wires, sheets, rods and flowers[6-9]. It was proposed that reducing the material particles dimensions through preparation of nanosized materials can shorten the Li-ion diffusion distances, enlarge the electrode/electrolyte interface contact area, retard the volume changes upon Li^+ insertion/extraction, and promote prolonged and stable battery operation[10].

Recently, the free-standing composite electrodes with three-dimensional structure have attracted great attention, because of their excellent structural flexibility, enhanced electrical contact with metal current collector and shortened path length for Li^+ transport, which allowed for achieving more attractive electrochemical performance compared with the electrodes made from granular powders[11,12].

In the present work, we introduce a simple strategy to synthesize ZnO nanorods by growing them directly on copper foil substrate via hydrothermal method without using any templates. The electrochemical performance and structure of obtained binder-free ZnO nanorods as electrode for lithium-ion batteries have been investigated. Used in a lithium half-cell, the binder-free ZnO nanorods electrode exhibited a high reversible capacity of 402 mAh g^{-1} at a current density of 200 mA g^{-1} even after 100 cycles, demonstrating very attractive prospective for its application as anode for LIBs.

2. EXPERIMENTAL

Highly-aligned ZnO nanorods arrays on a copper foil were fabricated by a facile hydrothermal method[11]. The schematic of the fabrication process for ZnO@CF is shown in Fig. 1. Typically, 5 mM $Zn(CH_3COO)_2$ (99%, Sigma) was dissolved in ethanol and the solution was drop-cast onto copper foil, and the foil was heated under reduced pressure in a tube furnace at 350 °C for 20 min to yield a layer of ZnO crystal seeds on it. The copper foil was washed by acetone and ethanol. Further, the copper foil substrate with the seed layer was soaked in aqueous solution of 25mM $Zn(NO_3)_2$(99%,National Medicine) and 25mM methenamine (99%, National Medicine) at 90°C for 4 h. Finally, the foil was rinsed with deionized water for several times, and dried in a drying oven at 60 °C for 12 h, and the ZnO nanorods arrays on copper foil electrode were successfully prepared.

The structure of the as-prepared product was investigated by X-ray diffraction (XRD, Bruker D8 advance with Cu Kα radiation). The morphology of the material was characterized by field-emission scanning electron microscopy (FE-SEM, S4800) and transmission electron microscopy (TEM, JEM-2100F, JEOL). Elemental analysis was carried out by X-ray photoelectron spectroscopy (XPS, VGESCA-LAB MKII) with a monochromatic Mg Kα X-ray source.

Electrochemical properties of the prepared material were investigated using coin-type cells (CR2025) with lithium metal foil as both counter and reference electrodes at room temperature. The as-prepared ZnO nanorods arrays on copper foil were used directly as a binder-free working electrode. The cells were assembled in a glove box (MBraun) filled with Ar (99.9995 %). The electrodes were separated by a microporous polypropylene separator (Celgard 2300). The electrolyte was a mixed solution of 1M $LiPF_6$ dissolved in dimethyl carbonate, diethyl carbonate, and ethylene carbonate (DMC:DEC:EC=1:1:1 by volume). After sealing in the glove box the cells were aged for 12 h before the electrochemical measurements. A battery tester (Arbin BT-2000) was used to investigate the lithium cells cycling performance at various current densities within the cutoff voltage limits from 0.005 V to 3 V *vs.* Li^+/Li.

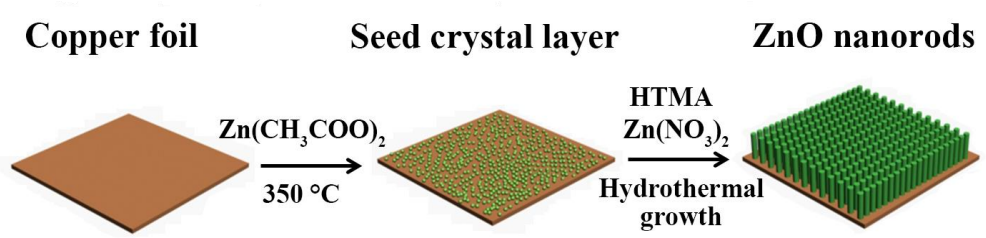

Figure 1. Schematic of the fabrication process for ZnO@CF.

3. RESULTS AND DISCUSSION

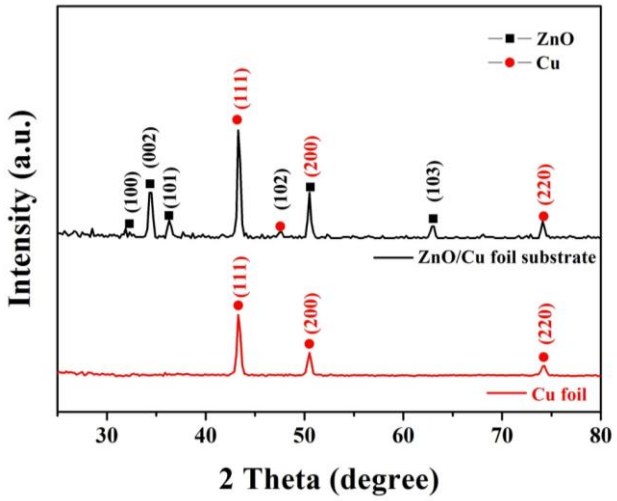

Figure 2. XRD patterns of ZnO@CF and naked Cu foil.

Fig. 2 shows the XRD pattern of the prepared ZnO nanorods arrays on copper foil substrate (ZnO@CF) and a naked copper foil substrate. The peaks appearing in the XRD spectra of ZnO@CF at 31.8°, 34.4°, 36.2°, 47.5°, and 62.9° correspond to the lattice planes of (100), (002), (101), (102) and (103) of hexagonal wurtzite structured ZnO (JCPDS, No. 36-1451), respectively [13-15]. The diffraction peaks of ZnO@CF at 43.6°, 50.5° and 74.5° can be indexed as the (111), (200) and (220) planes of copper (JCPDS, No. 04-0836). Except this, no impurity peaks were detected in the XRD patterns, which confirm the successful synthesis of high-purity ZnO grown on the copper foil substrate. The as-prepared ZnO@CF was further studied using XPS. Fig. 3 presents the XPS spectra of the Zn2p and O1s indicating the presence of Zn and O elements in the ZnO@CF sample. The strong peaks located at 1044.2 eV and 1021.1 eV (Fig. 3a) were assigned to Zn2p1/2 and Zn2p3/2, respectively. In the O1s spectrum, two different peaks situated at 531.47 eV and 530.11 eV (Fig. 3b) correspond to the binding energy of O-H and O-Zn, confirming formation of ZnO.

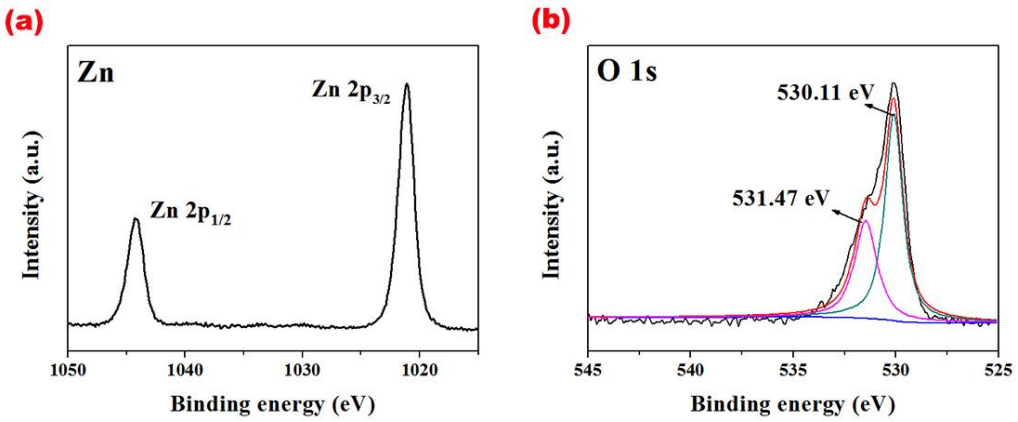

Figure 3. (a) Zn 2p XPS spectra and (b) O 1s XPS spectra of ZnO@CF**.**

The SEM and TEM images of the as-prepared ZnO nanorods are presented in Fig. 4. It can be seen from Fig. 4a that the ZnO nanorods arrays with 50-100 nm in diameter cover the copper foil substrate surface. This morphology assures good electrical contact of the active material with the copper current collector/substrate and provides enhanced interaction area at the electrode/electrolyte interface. The inset of Fig. 4b illustrates the diameter distribution of the ZnO nanorods derived from the SEM data in Fig. 4b. One can see that the ZnO nanorods have homogeneous diameter distribution with an average value of 72.7 nm. Such homogeneous nanostructured feature of the electrode could facilitate the charge transport, allowing for high energy density operation during the discharge/charge process[16,17]. The internal structure of ZnO nanorods were investigated by TEM. The low magnification TEM image of ZnO nanorods (inset of Fig. 4c) shows that the length of the nanorods is about 800nm, and the diameters are consistent with that obtained from the SEM data. From the HRTEM image of the as-prepared ZnO nanorods presented in Fig.4c, obvious interlayer distance of 0.248 nm could be observed, which agrees with the spacing of the (002) lattice plane of hexagonal ZnO, confirming the XRD results on preferred *c*-axis orientation of ZnO. The SAED patterns of the

nanorods in Fig. 4d reveal the single-crystalline nature of the as-prepared ZnO nanorod material. These results further confirm that vertically oriented ZnO nanorod arrays in single-crystalline phase have been successfully grown on the copper foil substrate via a facile hydrothermal method.

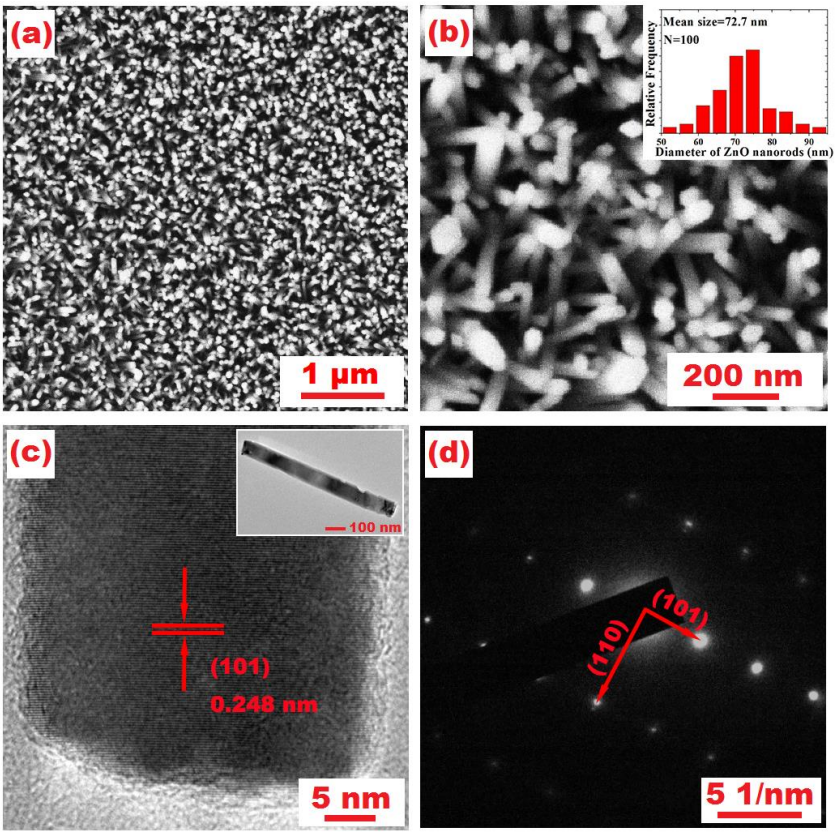

Figure 4. (a,b) SEM images and (c) HRTEM image of the ZnO nanorods; (d) SAED pattern of the the ZnO nanorods; the inset in (b) presents the diameter distribution of the ZnO nanorods based on the SEM images; the inset in (c) shows the lower magnification TEM image of the ZnO nanorods.

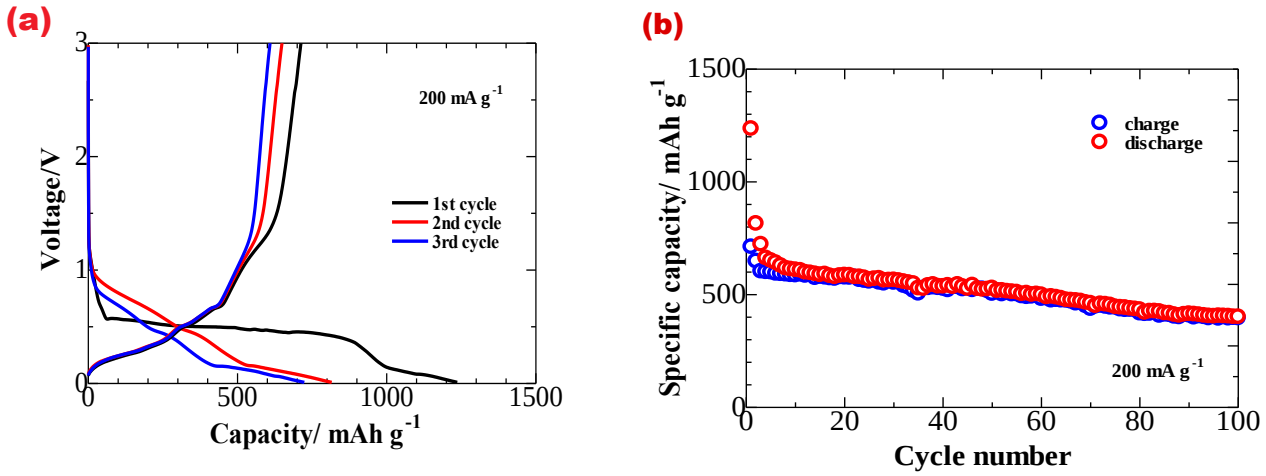

Figure 5. (a) The galvanostatic discharge/charge profiles of lithium cell with the ZnO@CF electrode; (b) Cycle performance of lithium cell with the ZnO@CF electrode for 100 cycles at 200 mA g^{-1}.

The results of galvanostatic charge/discharge tests of the ZnO@CF anode at a current density of 200 mA g^{-1} are presented in Fig. 5a. The first discharge curve shows an obvious plateau around 0.5-0.6V *vs.* Li^+/Li, corresponding to the reduction process of ZnO to Zn metal ($ZnO + 2Li \rightarrow Zn + Li_2O$) [13]. One can see the second voltage plateau at 0.2V appearing upon deep discharge, which is ascribed to the formation of lithium-zinc alloy ($xLi + Zn \rightarrow Li_xZn$). The initial discharge and charge capacities for the ZnO@CF anode were 1236 mAh g^{-1} and 712 mAh g^{-1}, respectively, with a corresponding coulombic efficiency of about 58%. This initial irreversible capacity loss and low coulombic efficiency is mainly associated with the inevitable process of formation of SEI [18]. In the following cycles, the similar charge/discharge curves imply the same Li-ion insertion/desertion and electron conduction process and highly reversible reaction.

The cycling performance of the ZnO@CF anode is recorded in Fig. 5b. It can be seen that the cell exhibits a capacity loss within a few initial cycles accompanied; cycle performance stabilizes upon further cycling delivering a capacity around 663 mAh g^{-1}. The ZnO@CF anode shows a good cycling stability with a reversible capacity of 402 mAh g^{-1} after 100 cycles; this performance enhancement could be attributed to the structural benefits of the ZnO@CF anode prepared in this work. The ZnO nanorods directly grown on the copper substrate provide vacant spaces to enable accommodation of large volume changes upon charge/discharge process, protecting the electrode from physical damage caused by swelling and shrinkage. Furthermore, the as-prepared free-standing ZnO@CF anode with 3D hierarchical structure is used directly without adding any polymeric binder, thereby avoiding any unwanted conductivity impairment and energy loss caused by the resistance of the binders.

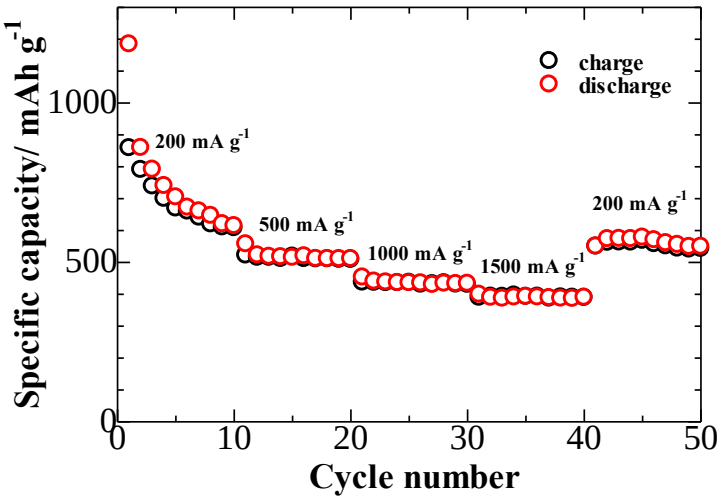

Figure 6. Rate capability of lithium cell with the ZnO@CF electrode.

The rate capability tests results, as depicted in Fig. 6, reveal an excellent high current density performance of the ZnO@CF electrodes. Ten galvanostatic charge/discharge cycles were carried out at various densities ranging from 200 to 1500 mA g^{-1}. The ZnO@CF electrode delivers high steady average discharge capacities of 615, 511, 434 and 390 mAh g^{-1} at the current densities of 200, 500, 1000 and 1500 mA g^{-1}, respectively. More importantly, when the current density was decreased back to 200 mA g^{-1}, the ZnO@CF electrode recovered its initial capacity of 550 mAh g^{-1} and sustained it

upon further cycling. This enhanced rate performance could be, again, attributed to the unique structure of the ZnO@CF anode, which provides large contact interfaces between electrode and electrolyte, facilitates charge transfer and, as a consequence, significantly improves charge-discharge capability of the system.

4. CONCLUSIONS

In summary, we developed a facile strategy to synthesize a free-standing ZnO@CF anode for LIBs with promising electrochemical performance. This synthetic route consists of a simple hydrothermal process resulting information/growth of the ZnO nanorods directly on copper foil substrates. This unique structure of a binder-free electrode provides spaces to accommodate large volume changes upon cycling and enlarged electrode/electrolyte interfaces for enhanced conditions for the charge and mass transfer in the system. Furthermore, the nanostructured features of the ZnO electrodes, synthesized in this work, effectively reduce the Li ions diffusion paths. These advantages result in high performance of the prepared ZnO@CF anode, which delivers a high reversible capacity of 402 mAh g^{-1} after 100 cycles, accounting for outstanding electrochemical behavior, and sowing its great potential as a promising high energy density anode for LIBs.

ACKNOWLEDGEMENTS
The authors acknowledge the financial support from the NSFC Grant No. 21406052, 51571094, Guangdong Province Grant NO. 2014A030308013, 2014B090915005, the Pearl River S&T Nova Program of Guangzhou (201506040045), the Program for the Outstanding Young Talents of Hebei Province (Grant No. BJ2014010), Scientific Research Foundation for Selected Overseas Chinese Scholars, Ministry of Human Resources and Social Security of China (Grant No. CG2015003002). ZB and YZ acknowledge the financial support by the grant from Nazarbayev University and the grant #4649/GF from the Ministry of Education and Science of Kazakhstan.

References

1. Y.P. Wu, E. Rahm and R. Holze, *J Power Sources*, 114 (2003) 228.
2. M.C. Qiu, L.W. Yang, X. Qi, J. Li and J.X. Zhong, *ACS Appl Mater Inter*, 2 (2010) 3614.
3. H.P. Li, Y. Li, Y.G. Zhang and C.W. Zhang, *J Nanopart Res*, 17 (2015) 370.
4. X.H. Huang, X.H. Xia, Y.F. Yuan and F. Zhou, *Electrochim Acta*, 56 (2011) 4960.
5. D. Bresser, F. Mueller, M. Fiedler, S. Krueger, R. Kloepsch, D. Baither, M. Winter, E. Paillard and S. Passerini, *Chem Mater*, 25 (2013) 4977.
6. M.A. Woo, T.W. Kim, I.Y. Kim and S.J. Hwang, *Solid State Ionics*, 182 (2011) 91.
7. A.D. Drozdov, *Acta Mech*, 225 (2014) 2987.
8. X.H. Huang, R.Q. Guo, J.B. Wu and P. Zhang, *Mater Lett*, 122 (2014) 82.
9. H.J. Yang, S.C. Lim, S.Y. He and H.Y. Tuan, *Rsc Adv*, 5 (2015) 33392.
10. S.K. Behera, *J Power Sources*, 196 (2011) 8669.
11. L.E. Greene, M. Law, D.H. Tan, M. Montano, J. Goldberger, G. Somorjai and P.D. Yang, *Nano Lett*, 5 (2005) 1231.
12. Y.Y. Wang, X.J. Jiang, L.S. Yang, N. Jia and Y. Ding, *ACS Appl Mater Inter*, 6 (2014) 1525.

13. H.P. Li, Y.Q. Wei, Y. Zhao, Y.G. Zhang, F.X. Yin, C.W. Zhang and Z. Bakenov, *J Nanomater*, 2016 (2016) 4675960.
14. X. Wang, L.Y. Huang, Y. Zhao, Y.G. Zhang and G.F. Zhou, *Nanoscale Res Let*, 11 (2016) 37.
15. H.P. Li, Y.Q. Wei, Y.G. Zhang, F.X. Yin, C.W. Zhang, G.K. Wang and Z. Bakenov, *Ionics*, (2016) doi: 10.1007/s11581-016-1661-x.
16. S.H. Zhao, J.X. Guo, F. Jiang, Q.M. Su, J. Zhang and G.H. Du, *J Alloy Compd*, 655 (2016) 372.
17. K.T. Park, F. Xia, S.W. Kim, S.B. Kim, T. Song, U. Paik and W.I. Park, *J Phys Chem* C, 117 (2013) 1037.
18. G.H. Zhang, H. Zhang, X. Zhang, W. Zeng, Q.M. Su, G.H. Du and H.G. Duan, *Electrochim Acta*, 186 (2015) 165.